

Enhancing the Mechanical and Fire-Resistant Properties of GFRP Composite using Boric Acid and Sodium Silicate Fillers

Tri Wibawa

Mechanical Engineering Department, Engineering Faculty, Sebelas Maret University, Indonesia | Industrial Engineering Department, Industrial Engineering Faculty, Universitas Pembangunan Nasional Veteran Yogyakarta, Indonesia
tri.wibawa@student.uns.ac.id

Kuncoro Diharjo

Mechanical Engineering Department, Engineering Faculty, Sebelas Maret University, Indonesia
kuncorodiharjo@ft.uns.ac.id (corresponding author)

Dody Ariawan

Mechanical Engineering Department, Engineering Faculty, Sebelas Maret University, Indonesia
dodyariawan@staff.uns.ac.id

Wijang Wisnu Raharjo

Mechanical Engineering Department, Engineering Faculty, Sebelas Maret University, Indonesia
m_asyain@staff.uns.ac.id

Cahyo Hadi Wibowo

Mechanical Engineering Department, Engineering Faculty, Sebelas Maret University, Indonesia
cahyohaw@student.uns.ac.id

Fathony Nada Saputro

Mechanical Engineering Department, Engineering Faculty, Sebelas Maret University, Indonesia
fathonysaputro@student.uns.ac.id

Andry Rakhman

Mechanical Engineering Department, Engineering Faculty, Sebelas Maret University, Indonesia
andrakhman@student.uns.ac.id

Aam Muharam

Research Center for Transportation Technology, National Research and Innovation Agency, Bandung, Indonesia
aamm001@brin.go.id

Sunarto Kaleg

Research Center for Transportation Technology, National Research and Innovation Agency, Bandung, Indonesia
suna024@brin.go.id

Abdul Hapid

Research Center for Transportation Technology, National Research and Innovation Agency, Bandung, Indonesia
abdu019@brin.go.id

Mohd Zulkefly

Fakulti Teknologi dan Kejuruteraan Mekanikal, Universiti Teknikal Malaysia Melaka, Malacca, Malaysia
zulkeflis@utem.edu.my

Received: 14 October 2024 | Revised: 31 October 2024 | Accepted: 3 November 2024

Licensed under a CC-BY 4.0 license | Copyright (c) by the authors | DOI: <https://doi.org/10.48084/etasr.9271>

ABSTRACT

This study investigates the effects of Boric Acid (BA), H_3BO_3 , and Sodium Silicate (SS), Na_2SiO_3 , as single fillers on the mechanical and fire-resistant properties of Glass Fiber Reinforced Polymer (GFRP) composites. Various compositions of BA and SS were incorporated into the GFRP matrix, and the resulting composites were analyzed using X-ray Diffraction (XRD), Fourier Transform Infrared Spectroscopy (FTIR), Scanning Electron Microscopy (SEM), Thermo-Gravimetric Analysis (TGA), and Differential Thermal Analysis (DTA). The results demonstrate that BA significantly enhances the amorphous structure and mechanical strength of GFRP composites, with optimal performance at 10% BA content. In contrast, SS improves thermal stability but reduces mechanical strength at higher concentrations due to agglomeration. Fire resistance testing revealed that both fillers increase the ignition time and decrease the burning rate, with BA exhibiting superior performance. These findings suggest that BA is a more effective filler for improving the mechanical and fire-resistant properties of GFRP composites, while SS can serve as a complementary additive to enhance thermal stability.

Keywords-GFRP composites; boric acid; sodium silicate; mechanical properties; fire resistance

I. INTRODUCTION

GFRP is extensively utilized across various industries, including aerospace, automotive, railway, electronics, and sports equipment [1]. The incorporation of Glass Fiber (GF) enhances the material's strength, stiffness, and resistance to fatigue and corrosion [2, 3]. Unsaturated Polyester Resin (UPR), employed as the matrix, provides good adhesion to the glass fibers and is a cost-effective solution. GFRP offers several advantages, such as a high strength-to-weight ratio, low production costs, and excellent performance [4]. However, GFRP is susceptible to damage from prolonged exposure to ultraviolet light, humidity, temperature fluctuations, rain, and fire [5, 6]. The material's flammability poses a challenge in certain applications. Fire resistance is crucial, as combustion involves fuel, oxygen, and heat [7-9]. The carbon chains in GFRP readily decompose when exposed to fire and oxygen, which can be mitigated by incorporating fire retardants. These retardants function by reducing fuel availability, limiting oxygen supply, and absorbing heat, thereby interrupting the combustion cycle, either at its onset or during its progression [10, 11]. Fire retardants in polymers serve three primary purposes: fuel reduction, oxygen inhibition, and heat absorption [12-14]. Certain fire retardants can also melt at high temperatures to form a protective layer, preventing further fire spread [15]. These properties make fire retardants essential for safety, as they are effective, non-toxic, and environmentally friendly. BA is a notable fire retardant frequently employed to safeguard flammable substances. As a fire-resistant coating, boric acid can enhance the fire-resistant properties of materials by penetrating wood and wood fibers [16]. Its porous structure

provides excellent thermal insulation, minimizing heat transfer and protecting the material from fire damage. This coating functions as an effective fire barrier, reducing material degradation [17, 18]. SS is another fire retardant that forms an insulating membrane layer, which decreases heat transfer and protects materials from damage. The addition of SS during composite manufacturing promotes the formation of polysilicate, creating a protective layer on the composite surface upon heat exposure, thereby enhancing the fire-resistant properties [19]. This ultimately results in improved product performance and fire resistance within the composite [20, 21]. Combining two or more flame-retardant materials can further enhance the fire resistance of composite materials. For instance, it was demonstrated that combining boric acid and Montmorillonite nanoclay (MMT) substantially improved the combustion resistance of composite materials, primarily due to BA's inherent fire-resistant properties [22]. While the addition of BA-MMT increased flexural strength, it resulted in a slight decrease in tensile strength. A study reported that incorporating 0.5% BA by weight yielded optimal improvements in tensile strength, shear strength, elastic modulus, shear modulus, and Poisson's ratio, with respective increases of 24.78%, 8.75%, 25.13%, 11.24%, and 12.5% [23]. However, the glass transition temperature (T_g) of the composite decreased with increasing BA content, reaching its lowest at a 1% concentration. Furthermore, interlayer delamination and matrix/fiber failure were observed in all samples. Hybrid materials with SS and polyisocyanate fillers, were explored, finding enhanced heat release rates, fire spread rates, decomposition rates, and increased residue and Limiting Oxygen Index (LOI) values

compared to rigid polyurethane materials [24]. The addition of Al_2O_3 and SiO_2 further enhanced the composite's thermal stability [25]. The flexural strength of the SiC_f/SiOC composite also increased with SS filler content; nevertheless, excessive SS reduced density and increased porosity by obstructing the infiltration path [26].

Previous studies have demonstrated the effectiveness of incorporating BA and SS fillers in mitigating the flammability issues of GFRP composites [27, 28]. However, the impacts of single fillers on the fire resistance and mechanical properties of GFRP composites remain underexplored. This research aims to address this knowledge gap by investigating the influence of single BA and SS fillers on the mechanical characteristics and fire resistance of GFRP composites.

II. MATERIALS AND METHODS

A. Material Preparation

This study employed orthophthalic UPR type 268 BQTN provided by Singapore Highpolymer Chemical Products (SHCP). The resin was cross-linked using Methyl Ethyl Ketone Peroxide (MEKP) with the MEPOXE brand produced by PT Kawaguchi Kimia Indonesia. E-glass Chopped Strand Mat (CSM) and Woven Roving (WR) fibers, type EMC200, from PT Makmur Fantawijaya Chemical Industries were utilized as reinforcement. The BA filler was supplied by Heansa Kimia, sieved to 200 mesh, and oven-dried at 125°C for 30 minutes to reduce moisture content. The SS solution was prepared by dissolving 10 wt% of silica-rich pumice particles in 2 M NaOH at 95°C for 2 hours under continuous stirring at 300 rpm. The solution was filtered to remove residues and impurities, then precipitated with 10 mL of ethanol and 5 M HNO_3 at 65°C and pH 7. The resulting silica gel was filtered, washed with hot distilled water to eliminate impurities, and dried at 80°C for 4 hours [29].

B. Composite Preparation

Composite materials were produced utilizing a combination of hand lay-up and compression molding procedures utilizing a release agent-coated glass mold with dimensions of $300 \times 200 \times 3.2$ mm for various compositions, including 70-80% UPR, 20% GF, and 0-10% fillers as shown in Table I.

TABLE I. COMPOSITION OF GFRP COMPOSITES

Sample	GF (% wt)	UPR (% wt)	BA (% wt)	SS (% wt)
C	20	80	-	-
CBA1	20	78	2	-
CBA2	20	76	4	-
CBA3	20	74	6	-
CBA4	20	72	8	-
CBA5	20	70	10	-
CSS1	20	78	-	2
CSS2	20	76	-	4
CSS3	20	74	-	6
CSS4	20	72	-	8
CSS5	20	70	-	10

The UPR and the filler were blended at 3000 rpm for 5 minutes, and the resulting mixture was left to remove all air bubbles. Additionally, the MEKP was added at 1% wt and

mixed at 3000 rpm for 1 minute to achieve a homogeneously filled matrix. The matrix was then poured into the mold and leveled across three layers of GF configuration (CSM-WR-CSM). Finally, the mold was covered with a coated glass and allowed to undergo a 24-hour curing process. The composite was subsequently removed from the mold and post-cured at 105°C for 60 minutes to ensure complete crosslinking and remove any residual moisture. All test specimens were prepared by cutting the GFRP composite into standard shapes for each test.

C. Characterization and Testing

The fracture surfaces of the composite material were characterized using a JEOL JCM-7000 SEM. TGA and DTA were performed on an STA PT 1600 instrument, with a heating rate of $20^\circ\text{C}/\text{min}$ from 30 to 600°C under a dry air atmosphere. FTIR was conducted using a Shimadzu IR Prestige-21 spectrometer, covering a wavenumber range of $400\text{-}4000\text{ cm}^{-1}$. XRD analysis was performed using a Bruker D8 Advance 3kW diffractometer equipped with a LynxEye XE-T detector and a Cu K-alpha radiation source. Macro-photography was utilized with a Canon DSLR EOS 700D camera, featuring an 18-55mm macro lens and an 18 MP CMOS sensor, to observe the fracture phenomena of the samples after impact and burn testing.

Composites were subjected to flexural strength testing using the three-point bending method in accordance to ASTM D790, which was carried out with a UTM JTM-UTS510 testing machine at a rate of 5 mm/min [30]. Additionally, the impact strength of the composites was evaluated through the Izod impact test method in accordance with ASTM D256, for unnotched specimen type [31]. Furthermore, the burning behavior of the composites, including the Burning Rate (BR) and Ignition Time (IT), was investigated by conducting testing according to ASTM D635, specifically the horizontal burning test [32].

III. RESULTS AND DISCUSSION

A. X-Ray Diffraction (XRD)

The XRD analysis indicates that the addition of BA and SS significantly modifies the amorphous diffraction pattern, as presented in Figure 1 and Table II. The control sample without any filler exhibits lower peak intensity and a broader distribution, suggesting a smaller amorphous size and lower degree of amorphousness. The peaks are observed in the range of $2\theta = 18^\circ$ to 30° , corresponding to an amorphous size of 7.65 nm and an amorphous degree of 0.439. These amorphous structures are attributed to the UPR present in the GFRP composites. The size and degree of amorphousness have a significant influence on the mechanical strength of polymer composites [33, 34]. A similar phenomenon was observed with the emergence of a new, strong diffraction peak near $2\theta = 16.0^\circ$ in GF/Polypropylene (PP) composites [35].

The addition of 2% and 10% BA resulted to a primary peak at $2\theta = 30^\circ$, along with additional peaks at $2\theta = 18^\circ$ and $2\theta = 20^\circ$. Notably, the 10% BA sample exhibited a remarkably sharp and dominant primary peak at $2\theta = 30^\circ$ aligning with a study that reported characteristic BA peaks at 14.5° and 28° [36]. The

significant increase in diffraction peak intensity suggests a larger amorphous domain size, 14.72 nm for 2% BA and 16.85 nm for 10% BA, and a higher degree of amorphousness, 0.673 for 2% BA and 0.785 for 10% BA, indicating that BA effectively enhances the structural properties of GFRP composites. This increased amorphousness results in a more ordered and tightly bound structure, which may potentially improve the mechanical strength and deformation resistance of the material [37].

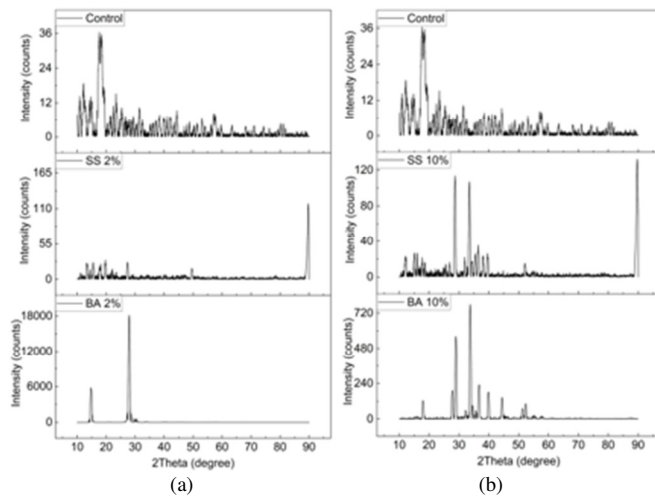


Fig. 1. XRD of single filler GFRP composite with variations in BA and SS composition: (a) 2% wt and (b) 10% wt.

TABLE II. DEGREE AND AVERAGE SIZE OF AMORPHOUS CRYSTALS ON GFRP COMPOSITES

Sample	Secondary to Primary Peak of 2θ	Degree of amorphous crystals (%)	Average size of amorphous crystals (nm)
C	18° to 30°	43.99	7.66
CBA1	18° to 30°	67.34	14.72
CBA5	20° to 30°	78.50	16.85
CSS1	22° to 30°	38.56	16.09
CSS5	22° to 30°	23.87	10.28

SS exhibits a primary peak at $2\theta = 30^\circ$ and a secondary peak around $2\theta = 22^\circ$. At a 10% SS, the primary peak remains at $2\theta = 30^\circ$ but with diminished intensity, accompanied by a minor additional peak at $2\theta = 22^\circ$ aligning with a study that observed a primary XRD peak around $2\theta = 27^\circ$. In contrast to BA, the incorporation of SS leads to an increase in the amorphous size, particularly at a concentration of 2% (16.09 nm). However, at a concentration of 10%, the amorphous size decreases to 10.27 nm [9]. This reduction in the amorphous size is accompanied by a lower degree of amorphousness, 0.238 for 10% SS, suggesting that SS does not achieve the same level of structural regularity as BA, which may negatively impact the mechanical properties of the composite. While the addition of SS at 2% enhances the amorphous size, the decrease in amorphousness at 10% indicates a less ordered structure, potentially rendering the material more susceptible to brittleness or reduced resistance to mechanical stress.

BA has been found to be more effective than SS in increasing the amorphous size and degree in GFRP composites, which in turn contributes to enhanced mechanical strength. As such, BA, particularly at a 10% concentration, represents a more optimal filler choice for improving the mechanical properties of GFRP composites. In contrast, while SS can increase the amorphous size, its impact on the degree of amorphousness is limited, potentially leading to reduced material strength when used at higher concentrations.

B. Fourier Transform Infrared Spectroscopy (FTIR)

Figure 2 presents the FTIR spectra for the control composite, without filler, and composites containing 2% BA and 2% SS. The control GFRP composite exhibits distinct peaks, including C-H stretching at 2937 cm^{-1} , C=O stretching at 1719 cm^{-1} , C-O stretching at 1264 cm^{-1} , and oxygen-silicon bonds in the Si-O-Si group of GF at 1059 cm^{-1} [38-40]. These peaks represent the functional groups of GF and UPR [41-42]. The composite with 2% BA filler displays a peak at 690 cm^{-1} corresponding to the deformation vibration of B-O bonds [43]. The band at 749 cm^{-1} is attributed to the vibration of the $[\text{BO}_3]_3$ structural group, the B-O-B bridge, or the vibration of atoms forming the $[\text{B}(\text{O},\text{OH})_4]$ tetrahedron [44]. Additional bands at 1059 , 1126 , and 1264 cm^{-1} arise from vibrations in the -O-B bonds of the orthoboric acid structure [45].

The peaks at 2017 and 2166 cm^{-1} are due to C-O stretching vibrations of adsorbed CO_2 , while the band at 2937 cm^{-1} indicates the presence of water in the 2% BA composite. These findings align with previous studies that have identified bands associated with boric acid functionality [46].

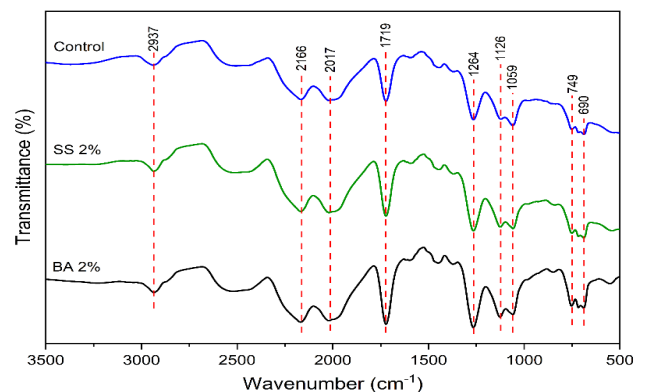


Fig. 2. FTIR of GFRP composites.

In the composite with 2% SS filler, a significant peak at 1126 cm^{-1} is related to Si-O stretching due to the presence of silica, indicating strong interaction with GFRP, which can enhance thermal and mechanical properties by strengthening the silicate network [47]. Other peaks, such as -OH stretching and SS bending at 2937 and 1719 cm^{-1} , exhibited reduced intensity. SS affects the interaction of ester groups in polyester, potentially reducing mechanical resistance at higher concentrations being consistent with other another study which analyzed functional groups in [48].

The FTIR analysis of the GFRP composite without filler indicated that BA and SS did not significantly alter the molecular structure of the composite. Additionally, the FTIR results revealed that the degree and size of amorphous regions did not impact the functional groups of GFRP composites, whether with BA or SS. BA contributed more to the formation of B-O bonds, enhancing fire resistance. Both fillers modified the functional groups of the composite, which could potentially improve mechanical and thermal properties. SS increased the Si-O interaction, thereby enhancing thermal and mechanical stability. However, excessive amounts of SS can compromise mechanical strength by disrupting the interconnections between polyester molecules.

C. Scanning Electron Microscopy (SEM) Observation

Physical properties such as the degree and size of amorphous crystals can influence the durability of composites, as evidenced by the fracture patterns observed after impact testing. The fracture behavior of the impact test samples was analyzed using surface morphology observations, as shown in Figure 3. Figure 3(a) illustrates a composite with a 2% BA concentration. Although BA can produce a relatively well-bound structure at low concentrations, some filler release is observed. This suggests that at lower concentrations, BA has a strong affinity with UPR, but its effectiveness in enhancing the mechanical strength of the composite is limited [49]. This is evident from the flexural and impact strength of composites containing 2% wt BA, which are lower than those with 10% wt BA. BA cannot form a sufficiently robust reinforcement network at low concentrations, resulting in filler release from the matrix under mechanical loading.

In contrast, the addition of 2% SS, as illustrated in Figure 3(c) enhances the interfacial bond and results in relatively uniform particle distribution. The matrix appears smooth, with sporadic filler agglomeration. The glass fiber is well embedded in the resin matrix, and the interfacial bond between GF, SS, and UPR appears cohesive, with minimal phase separation, indicating good adhesion properties and minimal fiber pull-out.

SEM images of composites with 10% BA, as shown in Figure 3(b), demonstrate that an increased filler concentration leads to a more organized and robust microstructure. The more pronounced amorphous crystal peaks in this material, as observed in previous XRD analysis, correlate with enhanced mechanical strength. At higher BA filler concentrations, the interaction between the filler and the matrix becomes more dominant, creating a more effective reinforcing network that enhances material strength [50].

However, in Figure 3(d) it is proposed that at a 10% SS concentration, the denser SS particles result in visible agglomeration and uneven distribution. The increased SS content causes visible voids and gaps at the fiber-matrix interface, indicating reduced adhesion and potential debonding under mechanical stress [51]. The increase in fiber pull-out observed in composites containing SS, without additional additives, leads to greater energy dissipation [52].

BA filler contributes positively to the mechanical strength of GFRP composites, as evidenced by the absence of phenomena indicating a reduction in mechanical properties.

This improvement is linked to an increase in the degree and size of amorphous crystals. BA is more effective in reinforcing the material structure by enhancing fiber-to-matrix adhesion, which in turn improves interlaminar strength [50]. While SS can improve interfacial bonding, it tends to produce a more brittle and amorphous structure, especially at higher concentrations.

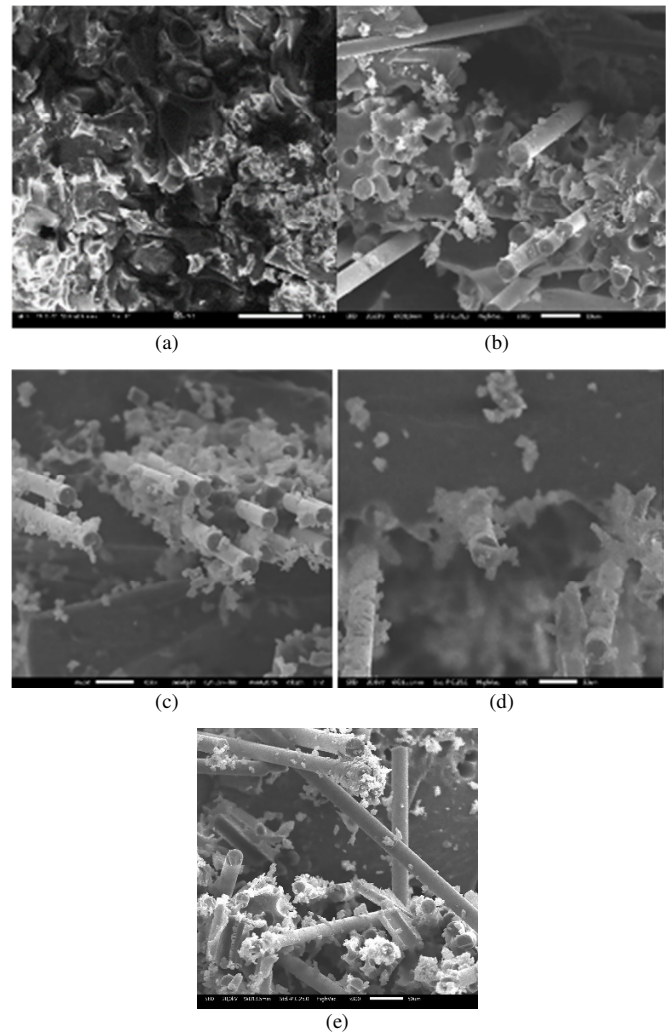


Fig. 3. SEM observation of fracture surface of impact test results on GFRP composites with (a) 0% filler (control), (b) 2% wt BA, (c) 10% wt BA, (d) 2% wt SS, (e) 10% wt SS.

D. Macro Observation of Impact Test Results

In addition to morphological observations with SEM, macro observations of the impact test fracture results can be used to validate the mechanical resistance of GFRP composites. Figure 4 presents samples obtained from impact tests using 2% and 10% wt of various fillers. Across all filler variations, a white area is observed between the fractures, representing the delamination zone. Delamination occurs as the composite withstands the applied load. The greater the composite's strength in resisting impact loads, the wider the delamination area [53]. Delamination typically occurs just

before fracture. The addition of filler can inhibit fracture propagation, reduce delamination, and minimize overall damage [54, 55].

In Figure 4(a), samples containing 2% BA, smaller cracks are concentrated in the central area of the sample. At low concentrations, BA begins to act as a filler, but it does not significantly enhance impact resistance. Impact strength increases as BA concentration rises. A concentration of 10% BA causes a noticeable color change in the sample, making delamination less visible. The resulting cracks appear more irregular compared to those in samples with other fillers. BA at 10% wt exhibits good interfacial bonding, causing the crack to propagate along alternative paths [56]. Strong chemical interactions between BA and the polymer matrix result in more uniform stress distribution and better energy dissipation during impact, thereby increasing the composite's overall impact strength [57, 58].

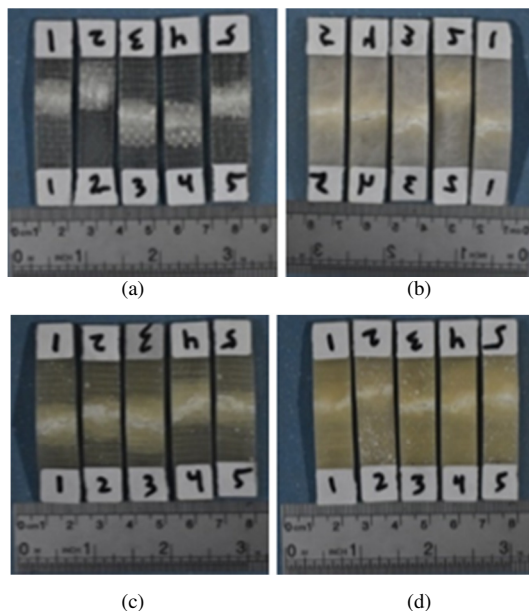


Fig. 4. Macro observation of impact test results on GFRP composites with (a) 2% wt BA, (b) 10% wt BA, (c) 2% wt SS, (d) 10% wt SS.

For SS at 2% wt, a significant improvement in impact strength is observed due to SS's effective stress distribution, which reduces particle agglomeration [59]. However, at 10% SS, more prominent cavities are visible, which facilitate crack formation and lead to composite failure due to SS particle agglomeration [60]. Composites with higher SS content tend to show reduced strength due to decreased matrix dispersion as silica content increases [20].

Overall, the increase in impact strength of GFRP composites with the addition of BA filler, as observed in SEM morphological studies, shows that BA effectively fills gaps, enhancing mechanical strength by filling cavities between layers. This is evidenced by the wider delamination and more irregular crack patterns, indicating good interfacial bonding, which forces cracks to seek alternative propagation paths. These results are associated with the increased degree and size

of amorphous crystals. In contrast, an increase in SS content up to 10% wt leads to particle agglomeration, resulting in cavities and widespread cracks, which deteriorate interlaminar bonding.

E. Thermo-Gravimetric Analysis (TGA) and Differential Thermal Analysis (DTA)

Unlike the previous physical properties that assess the mechanical resistance of GFRP composites, TGA and DTA were used to evaluate the heat characteristics of GFRP composites, which are closely related to their combustion resistance. Thermal characterization is illustrated in Figure 5 and Figure 6. The addition of 2% BA significantly increased the thermal stability of the composite compared to the control. A substantial mass loss begins around 350°C, indicating that BA acts as an effective flame retardant by slowing down the thermal degradation process. BA also significantly enhances thermal stability and, at specific concentrations, forms a protective barrier, reducing the peak heat release rate by more than 75% [22]. The addition of 10% BA further improves thermal resistance, with the primary degradation temperature occurring around 400°C and a larger residue remaining after testing. This suggests that higher BA concentrations not only increase thermal stability but also contribute to the formation of a protective layer during combustion, leaving more residue.

The addition of 2% SS showed slightly different results. Although the thermal stability of the SS composite was lower than that of the BA composite, it still outperformed the control. The primary thermal degradation occurred at a slightly lower temperature, but the significant remaining residue indicated the formation of an inorganic barrier layer due to the presence of SS. At a 10% SS concentration, thermal stability improved compared to 2%, though the remaining residue was less than that with 10% BA. SS tends to form a silica-based gel or barrier that degrades differently at high temperatures, explaining the variation in final residue amounts. SS forms an inorganic barrier during combustion, reducing flammability and increasing thermal stability [61].

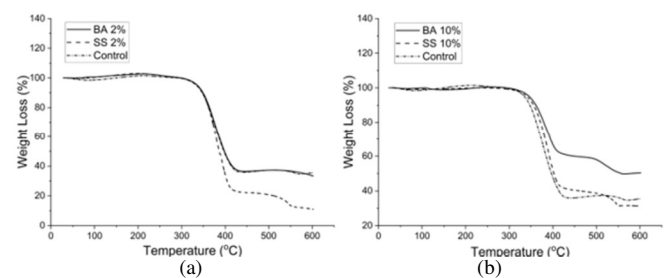


Fig. 5. TGA of single filler GFRP composite with variations in BA and SS composition: (a) 2% wt and (b) 10% wt.

Figure 6 demonstrates that the addition of BA and SS significantly alters the peak temperature and shape of the curve. This is due to interactions between the fillers and the polymer matrix, which affect thermal stability. At a 2% filler concentration, both BA and SS composites showed an earlier onset of degradation compared to the control sample, suggesting that low filler concentrations may act as catalysts for degradation. However, at a 10% concentration, the peaks

for both BA and SS shifted towards higher temperatures, indicating increased thermal stability at higher filler levels. The addition of inorganic fillers enhances thermal stability due to their intrinsic resistance to heat and the barriers they form against heat and mass transfer during decomposition [29].

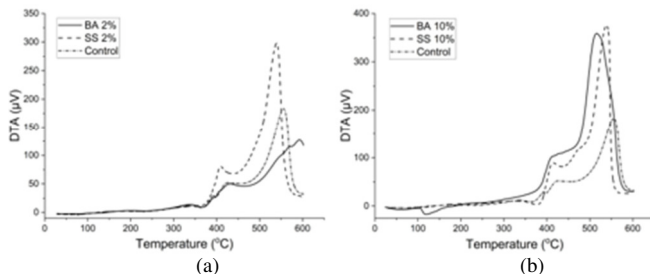


Fig. 6. DTA of single filler GFRP composite with variations in BA and SS composition: (a) 2% wt and (b) 10% wt.

F. Macro Observation of Burn Test Results

In addition to thermal characteristics, the fire resistance properties of GFRP composites with BA and SS fillers can be analyzed through observations of burned samples. Macro observations after burn tests are illustrated in Figure 7. BA releases water when heated, which helps cool the material and dilutes combustible gases. Conversely, SS forms a protective layer on the composite surface during heating, thereby isolating the polymer matrix from heat and flame penetration.

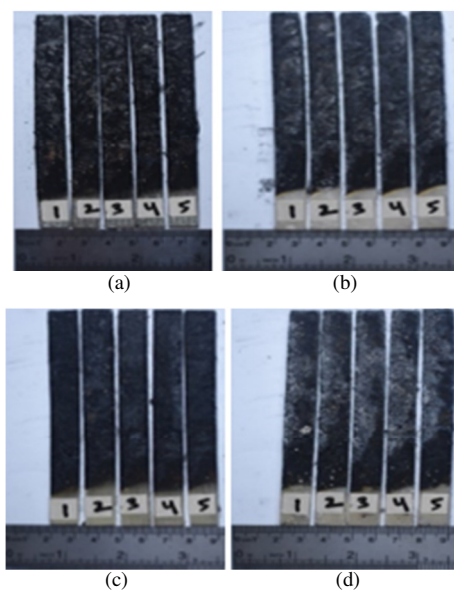


Fig. 7. Macro observation of the results of the GFRP composite burning test with (a) 0% filler (control), (b) 2% wt BA, (c) 10% wt BA, (d) 2% wt SS, (e) 10% wt SS.

Visual inspection revealed that samples with a 10% filler concentration exhibited better structural integrity compared to those with a 2% concentration, indicating that higher filler content significantly enhances fire resistance. These findings suggest the potential for using combined fillers to improve fire resistance in applications where material performance is

critical. This analysis is supported by several studies which found that GFRP composites with a combination of BA and SS exhibited increased fire resistance [29]. Increasing the BA content in GFRP composites resulted in a higher LOI, improved fire resistance, and reduced smoke density [22] suggesting a significant enhancement in fire resistance with higher BA content. Similarly, it was reported that composites treated with SS and boron compounds showed excellent fire resistance properties, primarily due to the formation of an insulating layer that reduces combustion and protects the underlying polymer matrix [62].

The results for 10% BA are closely related to the thermal resistance observed in the TGA/DTA analysis, where this concentration provides optimal improvements in both heat and fire resistance of GFRP composites. This is attributed to a higher level of dehydration, forming a more effective char layer that inhibits combustion. In contrast, SS enhances fire resistance by forming an intumescent layer on the surface, which prevents the GFRP composite from burning.

G. Mechanical Properties

Flexural strength measures a composite's ability to resist fracture under stress, ensuring its suitability and durability for various applications [63]. Figure 8 illustrates how filler type and weight fraction influence the flexural strength of GFRP composites. Different effects were observed depending on the filler composition: increasing BA content correlated with a rise in flexural strength. This finding is consistent with the study which reported a gradual increase in flexural strength with BA content up to 5% [64].

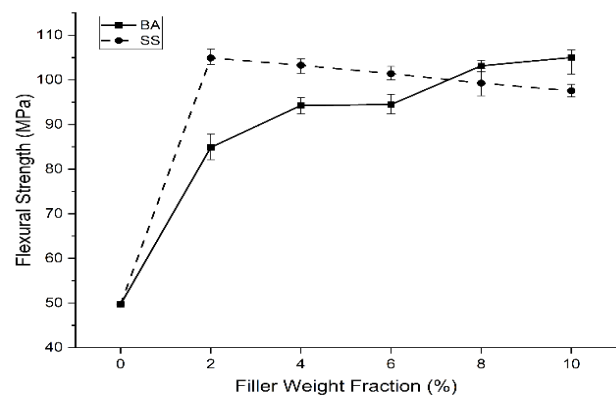


Fig. 8. Flexural strength of GFRP composite.

In contrast, SS showed an increase in strength only at 2 wt%, with a subsequent decline in flexural strength at higher concentrations. A similar trend was observed, with strength peaking at 10% composition and decreasing with further addition up to 30% [20]. Increasing the BA content from 2% to 10% progressively raised the flexural strength, peaking at 105 MPa at 10 wt% BA. This increase is attributed to BA's ability to reduce stress transfer and inhibit crack propagation [65]. The fine 200-mesh powder form of BA facilitates its integration into the fiber-resin interface, thereby enhancing composite strength aligning with the findings which showed increased

strength and fracture toughness at BA compositions up to 3% [66].

The addition of gel-form SS exhibited a different trend. An initial increase in flexural strength was observed at 2 wt% SS, but higher concentrations significantly reduced the strength, dropping to 97 MPa. This decline is attributed to the gel-like nature of SS, which inhibits bonding with the polyester matrix. As SS concentration increases, poor interaction with the matrix results in weak interfacial bonding [66]. Additionally, the high density and potential for agglomeration of SS further contribute to this reduction in strength [67]. This phenomenon is indicated by the presence of -OH groups in FTIR observations, which can interfere with the interaction between SS and UPR. Additionally, it was stated that high SS levels disrupt the cross-linking reaction between polycarboxylate and polyalcohol [20]. Particle size, shape, and concentration of components affect the flexural strength of the composite. Higher SS concentration can reduce strength due to agglomeration, while increased BA enhances amorphous crystals and strength. Cracks, delamination, and other phenomena observed further support these findings. Optimal BA content is around 10%, while SS concentrations above 2% decrease strength.

In addition to flexural strength, impact strength is a key indicator of the mechanical performance of GFRP composite materials. Impact strength reflects the material's capacity to withstand forces that can lead to failure. As seen in Figure 9, an increase in BA content correlates with increased impact strength; however, this trend with other studies which reported a decrease in impact strength beyond 2% BA composition [4, 68]. For SS filler, an increase in impact strength is observed at 2% content, followed by a decline at higher concentrations. This phenomenon was similarly reported in a study in which it was found that impact strength improved only at 2% SS and decreased thereafter [59]. The increase in impact strength in GFRP composites with BA addition is directly proportional to its concentration, starting at 2% BA with a value of 72 MPa and peaking at 81 MPa with 10% BA.

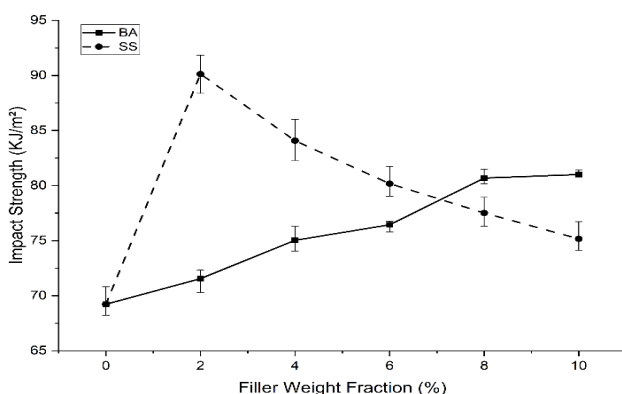


Fig. 9. Impact strength of GFRP composite.

Impact strength is positively correlated with flexural strength due to the reinforcing effect of random and woven GF, which enhances both flexural and impact properties. Additionally, BA acts as an effective filler, increasing strength

by filling voids between layers. This result differs from studies on PP composites, where higher BA percentages reduce strength due to plasticization, which weakens interfacial bonds [69, 70].

Similar to flexural strength, the optimum impact strength is achieved at 2% SS content. However, higher SS concentrations lead to decreased impact strength due to agglomeration caused by the gel form of SS, which creates local stress concentrations. This effect is also related to the presence of -OH groups that interfere with the bonding between SS and UPR. It was observed that SS content above 2% reduces impact strength due to the formation of barriers that inhibit stress transfer from the matrix to the fiber [59].

The observed pattern suggests a correlation between increased impact strength and flexural strength, attributed to the complementary roles of random GF, which enhances impact resistance, and woven GF, which contributes to flexural resistance. Consequently, each layer in the GFRP composite exhibits high mechanical resistance. Moreover, the optimal filling of voids by BA at higher concentrations leads to a gradual increase in strength, as confirmed by SEM observations. In contrast, while SS at 2% wt effectively transmits stress to the matrix and fibers, higher concentrations result in agglomeration, reducing impact strength.

H. Fire Resistance Properties

Ignition time and burning rate are two crucial parameters in assessing the fire resistance of composites. In Figure 10, both fillers increase the ignition time as their weight fraction rises, indicating enhanced fire resistance due to their flame-retardant properties. Across all concentrations, SS exhibits a higher ignition time compared to BA. While the ignition time increases with filler content for both fillers, BA shows a more linear trend, whereas SS demonstrates an exponential rise from 6% to 10%, suggesting a threshold effect where SS becomes particularly effective in slowing down the ignition process at higher concentrations.

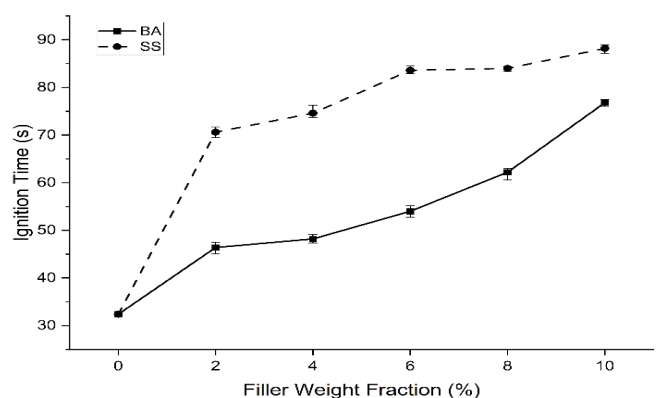


Fig. 10. Ignition time of GFRP composite.

Nevertheless, both BA and SS significantly increase ignition time compared to the composite without fillers. The flame-retardant effect of BA is corroborated by another study which found that combining 15 wt% BA with Multi-Walled

Carbon Nanotubes (MWCNT) increased the ignition time compared to samples with MWCNT alone [71]. The endothermic decomposition of BA, releasing water, cools the composite surface. Similarly, it was reported that SS reduces ignition time, extends the combustion process, and lowers the Peak Heat Release Rate (PHRR) by up to 40% compared to the sample without filler [24].

The combustion rate test results, illustrated in Figure 11, align with the ignition time findings. The addition of BA and SS fillers significantly reduced the combustion rate, with the most notable effect observed at 2% wt filler concentration. At this level, the burning rate dropped dramatically from 0.49 mm/s, without filler, to approximately 0.30 mm/s, representing a 33% decrease, indicating that even low filler concentrations can significantly improve the thermal resistance of composite materials.

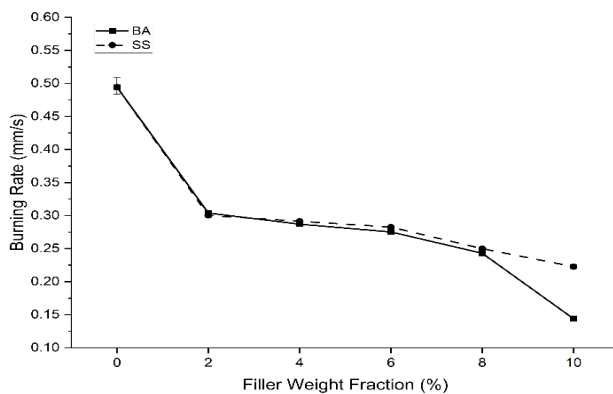


Fig. 11. Burning rate of GFRP composite.

At 2% concentration, BA and SS demonstrated similar effectiveness in reducing the burning rate. However, as the concentration increased to 4% and 6%, the burning rate decreased more gradually, reaching around 0.25 to 0.30 mm/s for both fillers. At 10% concentration, the performance difference became more pronounced. BA showed the most substantial reduction in burning rate, dropping to 0.14 mm/s, while SS only reduced the rate to 0.22 mm/s. This disparity is consistent with previous studies, where SS forms an intumescent layer during combustion, reducing the composite temperature and inhibiting fire spread. The intumescent layer in SS performs effectively, with an intumescent temperature around 195°C [72]. Conversely, BA forms a stronger char layer, as observed in microstructural analyses. BA melts at 236°C and dehydrates above 300°C, producing boron oxide, which forms a protective layer that inhibits flames [73]. The charring process increases with higher boric acid content [74].

BA and SS have proven effective in enhancing the fire resistance of GFRP composites [75, 76]. SS provides a moderate reduction in composite temperature and ignition time, while BA exhibits superior performance, particularly at higher concentrations. BA not only significantly reduces the burning rate but also forms a more robust protective layer, making it a superior choice for applications requiring high fire resistance.

IV. CONCLUSION

The addition of boric acid (BA) and sodium silicate (SS) significantly enhances the mechanical strength and fire resistance of Glass Fiber Reinforced Polymer (GFRP) composites. Employing multiple characterization techniques, including using X-ray Diffraction (XRD), Fourier Transform Infrared Spectroscopy (FTIR), Scanning Electron Microscopy (SEM), Thermogravimetric Analysis (TGA), and Differential Thermal Analysis (DTA), provides a comprehensive understanding of the filler-matrix interactions and their effect on composite properties. BA, particularly at a 10% concentration, effectively increases structural integrity, mechanical strength, and fire resistance. By promoting the formation of larger amorphous crystals, BA also improves interlaminar strength and impact resistance. Additionally, it enhances fire resistance through the formation of a protective char layer that inhibits combustion. Although SS contributes to thermal stability and heat transfer resistance, it can reduce mechanical strength at higher concentrations due to filler agglomeration and weaker matrix interaction. These findings highlight the potential of BA and SS for applications requiring both mechanical strength and thermal resistance.

ACKNOWLEDGMENT

The authors would like to thank the Ministry of Education, Culture, Research, and Technology, Indonesia, for funding this research from the Doctoral Research Grant through the applied research grant scheme (PDD Dikti 2024).

REFERENCES

- [1] M. Zainudin, K. Diharjo, M. Kaavessina, and D. Setyanto, "The properties degradation of exposed GFRP roof," *AIP Conference Proceedings*, vol. 1931, no. 1, Feb. 2018, Art. no. 030063, <https://doi.org/10.1063/1.5024122>.
- [2] G. Rathore and R. Seetharam, "Investigation of mechanical properties of glass fibre/SiC- B4C reinforced hybrid polymer composite," *Materials Today: Proceedings*, vol. 87, pp. 345–350, Aug. 2023, <https://doi.org/10.1016/j.matpr.2023.06.231>.
- [3] P. Morampudi, K. K. Namala, Y. K. Gajjala, M. Barath, and G. Prudhvi, "Review on glass fiber reinforced polymer composites," *Materials Today: Proceedings*, vol. 43, pp. 314–319, Mar. 2021, <https://doi.org/10.1016/j.matpr.2020.11.669>.
- [4] D. K. Rajak, P. H. Wagh, and E. Linul, "Manufacturing Technologies of Carbon/Glass Fiber-Reinforced Polymer Composites and Their Properties: A Review," *Polymers*, vol. 13, no. 21, Oct. 2021, Art. no. 3721, <https://doi.org/10.3390/polym13213721>.
- [5] A. E. Krauklis *et al.*, "Modelling of Environmental Ageing of Polymers and Polymer Composites—Modular and Multiscale Methods," *Polymers*, vol. 14, no. 1, Jan. 2022, Art. no. 216, <https://doi.org/10.3390/polym14010216>.
- [6] T. Lu, E. Solis-Ramos, Y. Yi, and M. Kumosa, "UV degradation model for polymers and polymer matrix composites," *Polymer Degradation and Stability*, vol. 154, pp. 203–210, Jun. 2018, <https://doi.org/10.1016/j.polymdegradstab.2018.06.004>.
- [7] J. Shen, J. Liang, X. Lin, H. Lin, J. Yu, and S. Wang, "The Flame-Retardant Mechanisms and Preparation of Polymer Composites and Their Potential Application in Construction Engineering," *Polymers*, vol. 14, no. 1, Dec. 2021, Art. no. 82, <https://doi.org/10.3390/polym14010082>.
- [8] Y. Kim, S. Lee, and H. Yoon, "Fire-Safe Polymer Composites: Flame-Retardant Effect of Nanofillers," *Polymers*, vol. 13, no. 4, Feb. 2021, Art. no. 540, <https://doi.org/10.3390/polym13040540>.

- [9] S. Araby, B. Philips, Q. Meng, J. Ma, T. Laoui, and C. H. Wang, "Recent advances in carbon-based nanomaterials for flame retardant polymers and composites," *Composites Part B: Engineering*, vol. 212, Feb. 2021, Art. no. 108675, <https://doi.org/10.1016/j.compositesb.2021.108675>.
- [10] N. S. Suharty, H. Ismail, K. Diharjo, D. S. Handayani, and W. A. Lestari, "Smart Natural Fiber Reinforced Plastic (NFRP) Composites Based On Recycled Polypropylene in The Presence Kaolin," in *IOP Conference Series: Earth and Environmental Science*, Solo, Indonesia, Apr. 2017, vol. 75, Art. no. 012026, <https://doi.org/10.1088/1755-1315/75/1/012026>.
- [11] K. Diharjo, V. B. Armunanto, and S. A. Kristiawan, "Tensile and burning properties of clay/phenolic/GF composite and its application," *AIP Conference Proceedings*, vol. 1717, no. 1, Mar. 2016, Art. no. 040024, <https://doi.org/10.1063/1.4943467>.
- [12] W. P. Raharjo, D. Ariawan, K. Diharjo, W. W. Raharjo, and B. Kusharjanta, "Fire Performance Enhancement of Natural-Fiber-Reinforced Polymer Composites," *New Approaches in Engineering Research*, vol. 15, pp. 48–72, Sep. 2021, <https://doi.org/10.9734/bpi/naer/v15/12992D>.
- [13] K. Diharjo, N. S. Suharty, A. E. B. Nusantara, and R. Afandi, "The Effect of Sokka Clay on the Tensile and Burning Properties of rPP/Clay Composite," *Advanced Materials Research*, vol. 1123, pp. 338–342, Aug. 2015, <https://doi.org/10.4028/www.scientific.net/AMR.1123.338>.
- [14] K. Diharjo, Y. Prasetya, M. Masykuri, and N. S. Suharty, "Fly ash/riposy composite: Inflammability on horizontal and surface burning," *AIP Conference Proceedings*, vol. 2262, no. 1, Sep. 2020, Art. no. 030009, <https://doi.org/10.1063/5.0021601>.
- [15] M. M. S. Mohd Sabeel *et al.*, "Flame Retardant Coatings: Additives, Binders, and Fillers," *Polymers*, vol. 14, no. 14, Jul. 2022, Art. no. 2911, <https://doi.org/10.3390/polym14142911>.
- [16] N. S. Suharty, I. Hanafi, K. Diharjo, M. Nizam, and M. Firdaus, "Improvement of Inflammability and Biodegradability of Bio-Composites Using Recycled Polypropylene with Kenaf Fiber Containing Mixture Fire Retardant," *Advanced Materials Research*, vol. 950, pp. 18–23, Jun. 2014.
- [17] A. Alizadeh, M. Geraei, and M. R. Mahoodi, "In situ fabrication of Al-Al₂O₃-TiB₂ hybrid nanocomposite; evaluating the effect of TiO₂ and B₂O₃ mechanical milling time on properties of composite created through vortex casting," *Materials Research Express*, vol. 6, no. 4, Jan. 2019, Art. no. 045037, <https://doi.org/10.1088/2053-1591/aafa61>.
- [18] J. Huang, W. Sun, Z. Zhang, Z. Ling, and X. Fang, "Thermal protection of electronic devices based on thermochemical energy storage," *Applied Thermal Engineering*, vol. 186, Mar. 2021, Art. no. 116507, <https://doi.org/10.1016/j.applthermaleng.2020.116507>.
- [19] P. Kiliaris and C. D. Papispyrides, "Polymer/layered silicate (clay) nanocomposites: An overview of flame retardancy," *Progress in Polymer Science*, vol. 35, no. 7, pp. 902–958, Jul. 2010, <https://doi.org/10.1016/j.progpolymsci.2010.03.001>.
- [20] M. F. Ahmad Rasyid, M. S. Salim, H. M. Akil, J. Karger-Kocsis, and Z. A. Mohd. Ishak, "Non-woven flax fibre reinforced acrylic based polyester composites: The effect of sodium silicate on mechanical, flammability and acoustic properties," *Express Polymer Letters*, vol. 13, no. 6, pp. 553–564, 2019, <https://doi.org/10.3144/expresspolymlett.2019.47>.
- [21] S.-N. Chen, P.-K. Li, T.-H. Hsieh, K.-S. Ho, and Y.-M. Hong, "Enhancements on Flame Resistance by Inorganic Silicate-Based Intumescent Coating Materials," *Materials*, vol. 14, no. 21, Nov. 2021, Art. no. 6628, <https://doi.org/10.3390/ma14216628>.
- [22] Y. Demirhan, R. Yurtseven, and N. Usta, "The effect of boric acid on flame retardancy of intumescent flame retardant polypropylene composites including nanoclay," *Journal of Thermoplastic Composite Materials*, vol. 36, no. 3, pp. 1187–1214, Mar. 2023, <https://doi.org/10.1177/08927057211052327>.
- [23] G. Örçen and D. Bayram, "Effects of Boric Acid on Laminated Composites: An Experimental Study," *Polymers*, vol. 16, no. 15, Jul. 2024, Art. no. 2133, <https://doi.org/10.3390/polym16152133>.
- [24] J.-J. Cheng and F.-B. Zhou, "Flame-retardant properties of sodium silicate/polyisocyanate organic-inorganic hybrid material," *Journal of Thermal Analysis and Calorimetry*, vol. 125, no. 2, pp. 913–918, Aug. 2016, <https://doi.org/10.1007/s10973-016-5454-2>.
- [25] M. A. Islam, M. A. Chowdhury, M. B. A. Shuvho, M. A. Aziz, and M. Kchaou, "Thermal analysis of hybrid composites reinforced with Al₂O₃ and SiO₂ filler particles," *Materials Research Express*, vol. 6, no. 12, Jan. 2020, Art. no. 125361, <https://doi.org/10.1088/2053-1591/ab6489>.
- [26] Z. Ren *et al.*, "Microwave absorption and mechanical properties of SiCf/SiOC composites with SiO₂ fillers," *Ceramics International*, vol. 47, no. 6, pp. 8478–8485, Feb. 2021, <https://doi.org/10.1016/j.ceramint.2020.11.214>.
- [27] M. Susilo, W. W. Raharjo, and K. Diharjo, "Inflammability of GFRP composite with the addition of aluminum tri-hydroxide, boric acid, and sodium silicate," *AIP Conference Proceedings*, vol. 2338, no. 1, Nov. 2021, Art. no. 040009, <https://doi.org/10.1063/5.0067006>.
- [28] T. Hapuarachchi and T. Peijs, "Aluminium trihydroxide in combination with ammonium polyphosphate as flame retardants for unsaturated polyester resin," *Express Polymer Letters - EXPRESS POLYM LETT*, vol. 3, no. 11, pp. 743–751, Oct. 2009, <https://doi.org/10.3144/expresspolymlett.2009.92>.
- [29] A. Rakhman, K. Diharjo, W. W. Raharjo, V. Suryanti, and S. Kaleg, "Improvement of Fire Resistance and Mechanical Properties of Glass Fiber Reinforced Plastic (GFRP) Composite Prepared from Combination of Active Nano Filler of Modified Pumice and Commercial Active Fillers," *Polymers*, vol. 15, no. 1, Dec. 2023, Art. no. 51, <https://doi.org/10.3390/polym15010051>.
- [30] *Standard Test Methods for Flexural Properties of Unreinforced and Reinforced Plastics and Electrical Insulating Materials*, American Society for Testing and Materials, West Conshohocken, PA, USA, 2003, <https://doi.org/10.1520/D0790-17.2>.
- [31] *Standard Test Method for Determining the Izod Impact Strength of Plastics*, American Society for Testing and Materials, West Conshohocken, PA, USA, 2000.
- [32] *Standard Test Method for Rate of Burning and/or Extent and Time of Burning of Plastics in a Horizontal Position*, American Society for Testing and Materials, West Conshohocken, PA, USA, 2022, <https://doi.org/10.1520/D0635-18.10.1520/D0635-22>.
- [33] S. Akbari, A. Root, M. Skrifvars, S. K. Ramamoorthy, and D. Åkesson, "Novel Bio-based Branched Unsaturated Polyester Resins for High-Temperature Applications," *Journal of Polymers and the Environment*, vol. 32, no. 5, pp. 2031–2044, May 2024, <https://doi.org/10.1007/s10924-023-03112-5>.
- [34] V. Fakhri, C.-H. Su, M. T. Dare, M. Bazmi, A. Jafari, and V. Pirouzfard, "Harnessing the power of polyol-based polyesters for biomedical innovations: synthesis, properties, and biodegradation," *Journal of Materials Chemistry B*, vol. 11, no. 40, pp. 9597–9629, Oct. 2023, <https://doi.org/10.1039/D3TB01186K>.
- [35] Y. Wang, L. Cheng, X. Cui, and W. Guo, "Crystallization Behavior and Properties of Glass Fiber Reinforced Polypropylene Composites," *Polymers*, vol. 11, no. 7, Jul. 2019, Art. no. 1198, <https://doi.org/10.3390/polym11071198>.
- [36] M. S. Bingöl and M. Çopur, "Determination of optimum conditions for boric acid production from coemanite by using co₂ in high-pressure reactor," *Journal of CO₂ Utilization*, vol. 29, pp. 29–35, Jan. 2019, <https://doi.org/10.1016/j.jcou.2018.11.005>.
- [37] N. Chousidis, "Polyvinyl alcohol (PVA)-based films: insights from crosslinking and plasticizer incorporation," *Engineering Research Express*, vol. 6, no. 2, May 2024, Art. no. 025010, <https://doi.org/10.1088/2631-8695/ad4cb4>.
- [38] J. Rusmirović *et al.*, "Fireproof phosphorylated kraft lignin/polyester based composites: Green material for rocket propellant thermal protection systems," *Scientific Technical Review*, vol. 69, no. 1, pp. 16–22, 2019, <https://doi.org/10.5937/str1901016R>.
- [39] H. Khakbaz, A. P. Basnayake, A. K. A. Harikumar, M. Firouzi, D. Martin, and M. Heitzmann, "Tribological and mechanical characterization of glass fiber polyamide composites under hydrothermal aging," *Polymer Degradation and Stability*, vol. 227, Jul. 2024, Art. no. 110870, <https://doi.org/10.1016/j.polymdegradstab.2024.110870>.

- [40] A. J. Bonon, M. Weck, E. A. Bonfante, and P. G. Coelho, "Physicochemical characterization of three fiber-reinforced epoxide-based composites for dental applications," *Materials Science & Engineering, C, Materials for Biological Applications*, vol. 69, pp. 905–913, Dec. 2016, <https://doi.org/10.1016/j.msec.2016.07.002>.
- [41] N. Koto and B. Soegijono, "Effect of Rice Husk Ash Filler of Resistance Against of High-Speed Projectile Impact on Polyester-Fiberglass Double Panel Composites," in *Journal of Physics: Conference Series*, Banten, Indonesia, Nov. 2019, vol. 1191, Art. no. 012058, <https://doi.org/10.1088/1742-6596/1191/1/012058>.
- [42] S. Yang, W. Liu, Y. Fang, and R. Huo, "Influence of hygrothermal aging on the durability and interfacial performance of pultruded glass fiber-reinforced polymer composites," *Journal of Materials Science*, vol. 54, no. 3, pp. 2102–2121, Oct. 2018, <https://doi.org/10.1007/s10853-018-2944-6>.
- [43] E. F. Medvedev and A. Sh. Komarevskaya, "IR spectroscopic study of the phase composition of boric acid as a component of glass batch," *Glass and Ceramics*, vol. 64, no. 1, pp. 42–46, Jan. 2007, <https://doi.org/10.1007/s10717-007-0010-y>.
- [44] B. Nayak, S. Srivastava, A. K. Singh, and S. K. Behera, "Influence of high energy milling on powder morphology and photoluminescence behavior of Eu-doped YBO₃ material," *Materials Chemistry and Physics*, vol. 254, Nov. 2020, Art. no. 123429, <https://doi.org/10.1016/j.matchemphys.2020.123429>.
- [45] B. Fuchs *et al.*, "Crystal structure re-determination, spectroscopy, and photoluminescence of π -YBO₃:Eu³⁺," *Zeitschrift für anorganische und allgemeine Chemie*, vol. 647, no. 22, pp. 2035–2046, Sep. 2021, <https://doi.org/10.1002/zaac.202100229>.
- [46] I. P. Kostova, T. A. Eftimov, K. Hristova, S. Nachkova, S. Tsoneva, and A. Peltekov, "An Effect of Boric Acid on the Structure and Luminescence of Yttrium Orthoborates Doped with Europium Synthesized by Two Different Routines," *Crystals*, vol. 14, no. 6, Jun. 2024, Art. no. 575, <https://doi.org/10.3390/cryst14060575>.
- [47] B. Feng and X. Luo, "The solution chemistry of carbonate and implications for pyrite flotation," *Minerals Engineering*, vol. 53, pp. 181–183, Jan. 2013, <https://doi.org/10.1016/j.mineng.2013.08.007>.
- [48] M. Wang *et al.*, "Selective Adsorption of Sodium Silicate on the Surface of Bastnaesite and Fluorite in Salicylhydroxamic Acid System under Alkaline Conditions," *Minerals*, vol. 13, no. 1, Dec. 2022, Art. no. 69, <https://doi.org/10.3390/min13010069>.
- [49] A. O. Ogah, O. E. Ezeani, F. O. Ohoke, and I. I. Ikelle, "Effect of nanoclay on combustion, mechanical and morphological properties of recycled high density polyethylene/marula seed cake/organo-modified montmorillonite nanocomposites," *Polymer Bulletin*, vol. 80, no. 1, pp. 1031–1058, Nov. 2022, <https://doi.org/10.1007/s00289-022-04574-8>.
- [50] E. Haincová and P. Hájková, "Effect of Boric Acid Content in Aluminosilicate Matrix on Mechanical Properties of Carbon Prepreg Composites," *Materials*, vol. 13, no. 23, Nov. 2020, Art. no. 5409, <https://doi.org/10.3390/ma13235409>.
- [51] G. Vara Prasad, S. Nagappa, Y. Ravi Kanth, I. Gopi Lakshmi, and J. Babu Rao, "Effect of brachyura shell particles on glass fibre reinforced epoxy polymer composite," in *Materials Today: Proceedings*, Jan. 2021, vol. 42, pp. 555–562, <https://doi.org/10.1016/j.matpr.2020.10.521>.
- [52] W. A. Taqwim, K. Diharjo, B. Kusharjanta, and A. Rakhman, "Effect of Pumice-Based Nanosilica and Sodium Silicate Addition on Impact Strength of GFRP Composite," presented at the 4th Borobudur International Symposium on Science and Technology, Nov. 2023, pp. 174–181, https://doi.org/10.2991/978-94-6463-284-2_21.
- [53] R. B. Ladani, A. T. T. Nguyen, C. H. Wang, and A. P. Mouritz, "Mode II interlaminar delamination resistance and healing performance of 3D composites with hybrid z-fibre reinforcement," *Composites Part A: Applied Science and Manufacturing*, vol. 120, pp. 21–32, May 2019, <https://doi.org/10.1016/j.compositesa.2019.02.010>.
- [54] M. R. Wisnom, "The role of delamination in failure of fibre-reinforced composites," *Philosophical Transactions of the Royal Society A: Mathematical, Physical and Engineering Sciences*, vol. 370, no. 1965, pp. 1850–1870, Apr. 2012, <https://doi.org/10.1098/rsta.2011.0441>.
- [55] B. Hulugappa, M. V. Achutha, and B. Suresha, "Effect of Fillers on Mechanical Properties and Fracture Toughness of Glass Fabric Reinforced Epoxy Composites," *Journal of Minerals and Materials Characterization and Engineering*, vol. 4, no. 1, pp. 1–14, Jan. 2016, <https://doi.org/10.4236/jmmce.2016.41001>.
- [56] T. Aydın, K. Turan, and N. Y. Sarı, "Investigation of Mechanical And Tribological Properties of Boric Acid Reinforced Composite Plates," *European Journal of Technique (EJT)*, vol. 11, no. 2, pp. 264–269, Dec. 2021, <https://doi.org/10.36222/ejt.923954>.
- [57] J. Zhang, L. Cao, and Y. Chen, "Mechanically robust, self-healing and conductive rubber with dual dynamic interactions of hydrogen bonds and borate ester bonds," *European Polymer Journal*, vol. 168, Mar. 2022, Art. no. 111103, <https://doi.org/10.1016/j.eurpolymj.2022.111103>.
- [58] N. M. Nurazzi *et al.*, "A Review on Mechanical Performance of Hybrid Natural Fiber Polymer Composites for Structural Applications," *Polymers*, vol. 13, no. 13, Jun. 2021, Art. no. 2170, <https://doi.org/10.3390/polym13132170>.
- [59] Md. T. Hossain, Md. S. Hossain, M. B. Uddin, R. A. Khan, and A. M. S. Chowdhury, "Preparation and characterization of sodium silicate-treated jute-cotton blended polymer-reinforced UPR-based composite: effect of γ -radiation," *Advanced Composites and Hybrid Materials*, vol. 4, no. 2, pp. 257–264, Jul. 2021, <https://doi.org/10.1007/s42114-020-00162-4>.
- [60] K. Kushwanth Theja, G. Bharathiraja, V. Sakthi Murugan, and A. Muniappan, "Evaluation of mechanical properties of tea dust filler reinforced polymer composite," *Materials Today: Proceedings*, vol. 80, pp. 3208–3211, Apr. 2023, <https://doi.org/10.1016/j.matpr.2021.07.213>.
- [61] K. M. A. Uddin, M. Ago, and A. Ferrer, "Hybrid films of chitosan, cellulose nanofibrils and boric acid: Flame retardancy, optical and thermo-mechanical properties," *Carbohydrate Polymers*, vol. 177, pp. 13–21, Dec. 2017, <https://doi.org/10.1016/j.carbpol.2017.08.116>.
- [62] T. Furuno, T. Goto, and S. Kato, "Combinations of Wood and Silicate, IX. EPMA Observation of Wood-Mineral Composites Using the Silicate-Boron Compound System and Estimation of Fire Resistance by Oxygen Index Method," *Journal of the Society of Materials Science*, vol. 50, no. 4, pp. 383–390, Apr. 2001, <https://doi.org/10.2472/jmsms.50.383>.
- [63] T. Subhani, "Microstructure and Mechanical Properties of Carbon Fiber Phenolic Matrix Composites containing Carbon Nanotubes and Silicon Carbide," *Engineering, Technology & Applied Science Research*, vol. 14, no. 2, pp. 13637–13642, Apr. 2024, <https://doi.org/10.48084/etasr.7070>.
- [64] A. Ardin, S. Sy, and S. Sofyan, "Effect of boric acid on the preservation of palm replanting wood waste," in *Journal of Physics: Conference Series*, Padang, Indonesia, Mar. 2021, vol. 1940, Art. no. 012085, <https://doi.org/10.1088/1742-6596/1940/1/012085>.
- [65] A. Bilgin, H. Gökmeşe, and B. Bostan, "Production of electro porcelain reinforced with boric acid and investigation of its properties," *Journal of the Faculty of Engineering and Architecture of Gazi University*, vol. 30, no. 4, 2015.
- [66] A. K. Ozdemir, D. Ozdemir Dogan, F. Tugut, H. Demir, and H. Akin, "Effects of boron on the mechanical properties of polymethylmethacrylate denture base material," *European Oral Research*, vol. 55, no. 1, pp. 45–53, Jan. 2021, <https://doi.org/10.26650/eor.20210132>.
- [67] N. S. Said, I. F. Olawuyi, and W. Y. Lee, "Pectin Hydrogels: Gel-Forming Behaviors, Mechanisms, and Food Applications," *Gels*, vol. 9, no. 9, Sep. 2023, Art. no. 732, <https://doi.org/10.3390/gels9090732>.
- [68] H. Ünal, S. H. Yetgin, and S. Köse, "Determination of mechanical performance of boric acid filled polypropylene based polymer composites," *Journal of Scientific Reports-A*, no. 055, pp. 185–192, Dec. 2023, <https://doi.org/10.59313/jsr-a.1354200>.
- [69] B. C. Ray, "Temperature effect during humid ageing on interfaces of glass and carbon fibers reinforced epoxy composites," *Journal of Colloid and Interface Science*, vol. 298, no. 1, pp. 111–117, Jun. 2006, <https://doi.org/10.1016/j.jcis.2005.12.023>.
- [70] C. Tsenoglou, S. Pavlidou, and C. Papaspyrides, "Evaluation of Interfacial Relaxation Due to Water Absorption in Fiber-Polymer Composites," *Composites Science and Technology*, vol. 66, no. 15, pp. 2855–2864, Apr. 2006, <https://doi.org/10.1016/j.compscitech.2006.02.022>.

- [71] O. B. Nazarenko, Y. A. Amelkovich, A. G. Bannov, I. S. Berdyugina, and V. P. Maniyan, "Thermal Stability and Flammability of Epoxy Composites Filled with Multi-Walled Carbon Nanotubes, Boric Acid, and Sodium Bicarbonate," *Polymers*, vol. 13, no. 4, Feb. 2021, Art. no. 638, <https://doi.org/10.3390/polym13040638>.
- [72] R. G. Puri and A. S. Khanna, "Intumescent coatings: A review on recent progress," *Journal of Coatings Technology and Research*, vol. 1, no. 14, pp. 1–20, Aug. 2016, <https://doi.org/10.1007/s11998-016-9815-3>.
- [73] X. Hou, Z. Li, and Z. Zhang, "Selectively Producing Acetic Acid via Boric Acid-Catalyzed Fast Pyrolysis of Woody Biomass," *Catalysts*, vol. 11, no. 4, Apr. 2021, Art. no. 494, <https://doi.org/10.3390/catal11040494>.
- [74] A. Donmez Cavdar, F. Mengeloğlu, and K. Karakus, "Effect of boric acid and borax on mechanical, fire and thermal properties of wood flour filled high density polyethylene composites," *Measurement*, vol. 60, pp. 6–12, Jan. 2015, <https://doi.org/10.1016/j.measurement.2014.09.078>.
- [75] J. Grzybek, M. Nazari, M. Jebrane, N. Terziev, A. Petutschnigg, and T. Schnabel, "Enhancing fire safety and thermal performance: Wood composites with bio-based phase change materials and fire retardants for building applications," *Fire and Materials*, vol. 48, no. 8, pp. 838–846, 2024, <https://doi.org/10.1002/fam.3238>.
- [76] V. Shree, A. K. Sen, S. Basu, and D. Ratna, "Use of a combination of phosphorous-containing epoxy resin and silica fillers for development of flame retardant thermoset polymer composites," *Journal of Vinyl and Additive Technology*, vol. 29, no. 1, pp. 130–143, Oct. 2022, <https://doi.org/10.1002/vnl.21949>.